Seasonality, land use, and diversity shape microbiome-pathogen interactions in wild populations of *Arabidopsis thaliana*

Authors: Henry LP[1,2*], Rat A[1,2,3], Laderman E[1,2], Lion R[4], Mayjonade B[4], TEAM PATHOCOM, Roux F[4], Weigel D[5,6], Bergelson J[1,2].*

[1]Department of Biology, New York University, New York USA
[2]Center for Genomics and Systems Biology, New York University, New York, USA
[3]RIBP-USC INRAE, Université de Reims Champagne-Ardenne, Reims, France
[4]LIPME, CNRS, INRAE, Université de Toulouse, Castanet Tolosan, France
[5]Department of Molecular Biology, Max Planck Institute for Biology Tübingen, Tübingen, Germany
[6]Institute for Bioinformatics and Medical Informatics, University of Tübingen, Tübingen, Germany

*Correspondence: LPH lph260@nyu.edu or JB jb7684@nyu.edu

TEAM PATHOCOM:
Department of Biology, New York University, New York USA
Tien-Hao Chang, Choghag Demijirian, Andrew Gloss, Hanna Märkle, Timothy C. Morton, Ankita Pandey, Kamal Radharamanan, Manmeet Singh, Hannah Whitehurst

Department of Molecular Biology, Max Planck Institute for Biology Tübingen, Tübingen
Haim Ashkenazy, Natalie Betz, Alejandra Duque, Martina Kolb, Ana Montalvão, Kevin Murray, Wei Yuan

LIPME, CNRS, INRAE, Université de Toulouse, Castanet Tolosan, France
Rémi Duflos, Paloma Duran, Irene Leccia, Alexandre Perrat, Sonia Silva

Unité Eco-Evo-Paleo, Université de Lille 1, CNRS, Villeneuve d'Ascq, France
Anne Duputié

***ACKNOWLEDGEMENTS*:** We thank L. Burkhardt, A. Contreras, S. Dambrowski, L. van Ess, K. Fritschi, A. Habring, C. Lino, M. Lucke, D. Lundberg, A. Marotz, E. Mehmetoğlu, A. Nowakoswki, G. Ofir, K. Romanova, R. Schwab, S. Stegmeyer, P. Sterr, L. Teasdale, S. Wang, F. Weber for assistance in the field and lab. We acknowledge the Zegar Family Foundation for their generous support of the NYU Genomics Core. LPH was supported by the Charles H. Revson Foundation. This work was funded by ERC project 951444/PATHOCOM awarded to FR, DW, and JB.

DATA AVAILABILITY: Code will be released upon publication. Sequences for samples will be deposited in NCBI SRA upon publication.

COMPETING INTERESTS: DW holds equity in Computomics, which advises plant breeders. DW also consults for KWS SE, a globally active plant breeder and seed producer. All other authors declare no competing interests.

ABSTRACT

The microbiome often protects plants against pathogens, but most findings are limited to controlled experiments in the lab. In the context of wild populations, one key challenge is to understand sources of variation that impact the commensal microbiome, which in turn shapes the degree of protection. Here, we surveyed both disease symptoms and microbiomes from wild populations of *Arabidopsis thaliana* over four consecutive seasons (fall/spring) across three different land use types. Land use types were stratified by anthropogenic influences and included forest meadows, human-impacted fields adjacent to agriculture or municipal parks, and highly disturbed habitats near railroad tracks. By building an integrative map of abiotic and biotic variables, we find that a key predictor of disease was biodiversity across ecological scales. Higher diversity plant communities reduced disease burden in *A. thaliana* populations but also increased diversity within the microbiome of *A. thaliana*. This increased microbial diversity was additionally associated with less disease in *A. thaliana*. However, the diversity-microbiome-disease relationships were all sensitive to season and further modulated by land use. Taken together, our work highlights the importance of anthropogenic change reshaping species interactions across ecological scales to impact disease risk in wild plant populations.

INTRODUCTION

Rapid anthropogenic change is reshaping ecological processes at multiple scales that can impact infectious disease dynamics [1–3]. As many abiotic and biotic factors are linked to anthropogenic change, the disturbance caused by these ecological and environmental changes is hypothesized to increase the emergence of novel pathogens [3,4]. Particularly for plants, anthropogenic land use change and its impact on neighboring ecological communities is expected to accelerate pathogen evolution [5]. If land use changes increase the degree of habitat fragmentation, increase plant density, and decrease community diversity, then disease risk can be amplified [3]. However, the risk of disease spread will depend on factors that impede or facilitate microbial transmission within and between plant species [3,5,6]. Identifying the multitude of ways that land use change impacts ecological interactions at different scales is essential to obtain insights into disease dynamics in plant populations undergoing rapid anthropogenic change.

The microbiome has emerged as an important factor in protecting plants against pathogens [7–9], offering potentially new approaches for combating emerging pathogens [10,11]. However, these findings are limited to controlled experiments in simplified ecological contexts. In realistic ecological contexts, plant disease dynamics are very different. Disease is often less severe in wild plants than in agricultural settings [12,13], and when disease outbreaks do occur, the incidence of coinfection is higher in wild populations [14]. While microbiomes are generally protective, interactions between the commensal microbiome and pathogen can instead lead to overall increases in pathogen diversity and burden [15,16]. Thus, microbiome-pathogen interactions potentially shape disease dynamics, but the impact remains poorly understood in naturalistic ecological contexts.

Understanding these complex microbiome-disease dynamics requires characterizing wild populations for both disease dynamics and microbiome variation. *Arabidopsis thaliana* is an

excellent model to investigate how land use change impacts microbial sharing because wild *A. thaliana* inhabits a broad range of environments and co-occurs with diverse assemblages of other plant species. We characterized the abiotic and biotic environments to identify drivers of microbiome variation and associations with disease in the phyllosphere. By sampling natural populations in different ecological contexts, we highlight the potential for land use types to reshape associations between microbiome variation and pathogen dynamics.

METHODS

Please refer to the supplement for full methodological details.

Site characterization and sample collection

Arabidopsis thaliana populations were sampled from 19 sites in southwest Michigan in the fall and spring between Fall 2021 and Spring 2023 (Fig. 1A, Supp. Table M1 for site details, dates, and sample sizes); we note that Site 17 was only sampled once and subsequently replaced with Site 19. As *A. thaliana* at these sites are winter annuals, collections were timed to start shortly after germination in November and harvesting was completed in the spring, after bolting reproductive stalks but before flowering and senescence. For each site, two transects were established to capture the range of micro-environmental variation, and each subsequent sampling returned to approximately the same transect locations within the site. For all analyses, data from both transects were pooled together to better partition variance at the site level.

We classified the land use type for sites into forest (N=7), anthropogenic (N=5), or railroad (N=7). Railroad sites were directly adjacent to active railroad tracks, while anthropogenic sites were often near agricultural fields or municipal parks. We used imperviousness data ([17]) to quantitatively distinguish forest and anthropogenic sites. Imperviousness data was determined at different spatial scales (every 50 m from 50-500 m, then 100 m up to 1 km). Forest sites were those with <5% imperviousness at all spatial scales, and the remaining non-railroad sites were classified as anthropogenic (Supp. Fig. M1); railroad sites had the highest imperviousness percentages at all spatial scales.

At each site, we characterized the abiotic environment relevant to plant-microbe interactions [18] using mean temperature on the day of sampling, cumulative precipitation in the three weeks preceding sampling, and the first two principal components of soil chemistry properties. Soil chemistry analysis was performed by A&L GreatLakes Laboratories. For the biotic environment, we focused on the companion plant community that co-occurs with *A. thaliana*. To further characterize companion plant communities at each sampling, two 50 cm x50 cm quadrats were placed in the approximate center of each transect, in areas with at least one *A. thaliana* individual within the quadrat. Percent coverage of the community was assessed using the quadrats. We then identified morphotypes as proxies for plant species, counted each morphotype, and saved a voucher for molecular identification using the chloroplast marker, *matK [19].* Community diversity was pooled from the two transects, and analyses used the genus-level *matK* assignment. Bray-Curtis dissimilarity was used to partition variance in compositional changes due to land use type, and Shannon diversity was used as the primary alpha-diversity measure in subsequent analyses.

We collected the above-ground rosettes of 16-24 *A. thaliana* individuals at each site per sampling period (N=1,327 plants total). The distribution of *A. thaliana* population size was approximated at a $\log_{10}$ scale. All plants were visually scored for the following disease symptoms [20]: chlorosis, necrosis, hypersensitive response (HR)-like lesions, *Albugo* presence, *Hyaloperonospora* presence, general fungal damage, and herbivory. A composite disease score (excluding herbivory) was built using the presence/absence of each symptom using principal components analysis. Other plant phenotypes measured were diameter, number of leaves, and bolting.

Approximately half of the *A. thaliana* samples were randomly selected to enrich for the endophytic portion of the microbiome in the field. Plants were briefly washed with 1X TE + 0.01% Triton-X, 80% ethanol, 2% bleach, and sterile water. Rosettes were blotted dry and placed immediately on dry ice until returned to the lab. We also collected a small portion of each non-*A. thaliana* morphotype to characterize the companion plant microbiome from pooled samples, as well as soil samples for microbiome characterization. Thus, microbiome analyses were focused on the three sample types: individual *A. thaliana* endophytes, companion plant pool, and soil.

Microbiome characterization

We characterized the *A. thaliana* microbiome using host-associated microbe PCR (hamPCR) [21] to simultaneously assess microbial load and community diversity (see supplement for full details). hamPCR co-amplifies a microbial marker gene with a single copy host gene in a single PCR reaction and then incorporates Illumina adapters for high-throughput sequencing. We used hamPCR for both bacteria (16S rRNA V5V6V7) and fungi (ITS1-2) with *GIGANTEA* as the host gene; the same amplicons were used for soil and companion plants without *GIGANTEA*. Microbial load is calculated by dividing the microbial reads by the *GIGANTEA* reads, and composition is determined using tools implemented in QIIME2 v2023.2 [22] and phyloseq [23]. ASVs were called using DADA2 [24] and taxonomically assigned using classify-sklearn Bayes classifier [25]. 16S rRNA were classified using the Greengenes database [26] and ITS sequences were classified using the Unite database [27]. Sequencing was performed on the Illumina NovaSeq platform, 1x300 bp at the NYU Genomics Core.

For the *A. thaliana* endophytes only, we assessed finer-scale phylogenetic resolution by developing primers that target strain diversity within *Sphingomonas* and other closely related genera (*mmdA* gene) and within the *Pseudomonas* genus (*HSD* gene). We chose to focus on these groups because *Sphingomonas* was the most abundant bacterial taxon and *Pseudomonas* contains both plant growth promoting strains [15] and important pathogens of *A. thaliana* as well as many other plants. *mmdA* and *HSD* amplicons were processed as stated previously for 16S rRNA and ITS, but taxonomy was assigned using a custom database. Sequencing was performed on the Illumina MiSeq platform, 1x300 bp at the NYU Genomics Core.

Statistical approach

We analyzed our data using mixed linear models and PERMANOVAs to identify associations between *A. thaliana* phenotypes (i.e., disease symptoms, microbiome variation) with environmental factors (see supplement for full details). For all mixed linear models, population was nested within the sampling year as a random effect. For PERMANOVAs assessing compositional differences (companion plant community and microbiome beta-diversity), population membership was used as blocks and year as a main term. For all microbiome beta-diversity analyses, we used a modified Aitchison distance [28]. While this distance metric is largely insensitive to read depth, we included read depth as a covariate, as rarefaction was not performed before ordination. Alpha-diversity metrics for all amplicons were rarefied to 1,000 reads for endophytes and 16,963 reads for companion plant and soil microbiomes (Supp. Fig. M2, supplemental methods for more detail). For models that focused only on endophytes (e.g., disease dynamics, microbial load and diversity), plant diameter was included as a fixed effect to control for differences in host size. As land use type and season often co-varied with many other factors, we primarily used these qualitative factors, but delineated when we used quantitative, site-level factors (e.g., companion plant community diversity, soil chemistry PC1, etc). We often tested for interactions between season and land use, but if interactions were not significant, the interaction terms were dropped. Mixed effects models were implemented in lme4 [29]. Residuals were assessed for dispersion, normality, and outliers using DHARMa [30]. Beta-diversity analyses used the adonis2 implementation of PERMANOVA in vegan [31] .

RESULTS

Land use shapes abiotic and biotic factors in A. thaliana populations

Across the 19 populations sampled, *A. thaliana* population sizes varied idiosyncratically across years and season, with no significant difference between land use types (Fig. 1B, Supp. Table R1). *Arabidopsis thaliana* plant size increased in the spring, again with no significant differences between land use type (Fig. 1C, Supp. Table R2).

We then characterized how abiotic and biotic factors vary across land use types for *A. thaliana* populations. For abiotic factors, we focused on temperature, precipitation, and soil chemistry. Neither temperature nor precipitation significantly differed between the land use types (Supp. Fig. R1, Supp. Table R3). Soil chemistry differed between land use types, where railroad soils were separated from anthropogenic and forest soils along PC1 (Supp. Fig. R2); railroad soils tended to have higher cation exchange capacity and organic matter levels.

For biotic factors, we characterized the co-occurring companion plant community, which potentially shares microbes with the focal *A. thaliana* individuals. The composition of companion plant communities was primarily structured by land use type ($R^2 = 0.09$, $F_{2,66} = 2.71$, $p=0.002$), with soil chemistry, temperature and year explaining marginal, but significant amounts of variance (Supp. Fig. R3, Supp. Table R5). The most abundant plants were *Arenaria* sp., *Cerastium* sp., and *Veronica* sp., as well as genera that were unique to each land use type (Supp. Fig. R3). Alpha-diversity of the companion plant community did not significantly differ across land use types or seasons (Supp. Fig. R4, Supp. Table R6). Taken together, the different land use categories are associated with different abiotic and biotic factors.

Land use modulates seasonal patterns of disease dynamics

We scored ~1,300 *A. thaliana* individuals for disease symptoms across the four sampling periods. The most frequently observed symptom was chlorosis, followed by HR-like lesions and necrosis (Fig. 2A). Many *A. thaliana* individuals often featured multiple disease symptoms, with the most common co-occurrence being chlorosis, HR-like, and necrosis. Notably, we detected a strong seasonal association for plants with multiple symptoms, with most plants in the spring exhibiting at least two different symptoms (Fig. 2B). More so, the dominant symptoms exhibited different temporal fluctuations in the different land use types (Supp. Fig. R5). For example, the presence of HR-like lesions decreased in the spring for forest populations, but increased for railroad populations; anthropogenic sites did not display seasonal dynamics for this symptom.

To understand how land use influences disease symptoms, we first integrated the different disease symptoms into a composite disease score using PCA loadings. PC1 separated the single- and multiple-symptom plants, and PC2 separated plants by symptom types (Supp. Fig. R6). With this composite score, we detected a significant three-way interaction between disease PC1 and land use, season, and Shannon diversity of the companion plant community (interaction Wald $X^2 = 33.3$, $p < 0.001$, Fig. 2C-D, Supp. Table R7). Forest populations exhibited increases in symptoms in the spring, and these swings were greater than in railroad populations (Fig. 2C). Populations at sites with strong anthropogenic influence, however, did not display a seasonal pattern. Companion plant community diversity was negatively correlated with disease PC1 across all land use types in the spring but only in the railroad populations during the fall (Fig. 2D). In the spring, the relationship between disease PC1 and companion plant diversity was steepest for anthropogenic sites. Overall, we find that the diversity of companion plants impacted disease symptoms in wild *A. thaliana,* but this impact was sensitive to land use and season.

Season strongly structures the endophytic microbiome of A. thaliana, but land use shapes microbial sharing with companion plants

We next assessed factors shaping microbial dynamics in *A. thaliana*. We explored three axes of variation in the bacterial and fungal microbiomes: 1) microbial load in *A. thaliana* endophytes, 2) the drivers of beta- and alpha-diversity differences between and within sample types, and 3) microbial sharing between *A. thaliana*, companion plants, and soil.

Microbial load of *A. thaliana* endophytes was significantly higher in the spring than in the fall for both bacteria and fungi (bacteria: $\beta = 0.89 \pm 0.04$ SE, $p < 0.0001$, fungi: $\beta = 0.16 \pm 0.07$ SE, $p = 0.02$, Fig. 3A-B, Supp. Table R8); more variance was explained for bacterial load (marginal $R^2 = 0.29$) than fungal load (marginal $R^2 = 0.01$). Bacterial and fungal loads were positively correlated ($\beta = 0.26 \pm 0.03$ SE, $p< 0.001$), although the strength of this correlation differed between fall and spring (interaction Wald $X^2 = 23.8971$, $p < 0.0001$, Supp. Fig. R7, Supp. Table R9). Land use did not significantly affect bacterial or fungal load.

Next, we focused on drivers of compositional differences between sample types. Most microbes were found across all sample types, but their relative abundance differed (Supp. Fig. R8 for bacteria, Supp. Fig. R9 for fungi); these microbes are also commonly observed in wild *A.*

thaliana populations [32–35]. Sphingomonadaceae were the most abundant bacteria across all sample types, while the most abundant fungal taxa varied (Table 1). Sample type only explained 8.1% of variance in bacterial microbiomes using a modified Aitchison distance metric ($F_{2,879}$ = 50.7, p = 0.001, Supp. Fig. R10, Supp. Table R10). Less variance was explained for fungal microbiomes, though sample type explained the most variance (R^2 = 0.04, $F_{2,760}$ = 14.8, p = 0.001, Supp. Fig. R10, Supp. Table R10). We note that other beta-diversity metrics explained less variance, but show qualitatively similar results (Supp. Fig R11, Supp. Table R11). Alpha-diversity was highest in soil and lowest in endophytes for both bacterial and fungal microbiomes (Supp. Fig. R12, Supp. Table R12).

While sample types generally shared the same microbes, different forces structured the microbiomes within each sample type. In these analyses, we included qualitative site descriptors (e.g., land use, season) as well as quantitative measures (e.g., companion plant community PC1, temperature, etc). Season structured beta-diversity in the endophytic bacterial microbiomes (R^2 = 0.28, $F_{1,743}$ = 349.3, p = 0.001) and companion plant microbiome (R^2 = 0.32, $F_{1,67}$ = 36.5, p = 0.001), while soil bacterial microbiomes were more strongly structured by land use (R^2 = 0.44, $F_{2,67}$ = 47.8, p = 0.001, Fig. 3C-D, Supp. Table R13). For fungal endophytes, season explained most of the little variation that could be explained (R^2 = 0.02, $F_{1,624}$ = 13.3, p = 0.001, Fig. 3E-F, Supp. Table R14). Like for bacteria, season structured the fungal microbiomes in companion plants (R^2 = 0.32, $F_{1,67}$ = 26.7, p = 0.001, Fig. 3E-F, Supp. Table R14). Other variables generally did not explain substantial variance structuring either bacterial or fungal microbiomes, with the exception that companion plant community PC1 explained significant variance in the soil bacterial community (R^2 = 0.14, $F_{1,67}$ = 30.7, p = 0.001, Fig. 3D-F, Supp. Table R13).

For alpha-diversity, we focused on the endophytes and expanded our dataset to include two additional amplicons, *mmdA* and *HSD*, which capture fine-scale diversity within *Sphingomonas* and *Pseudomonas*, respectively, allowing us to compare the response of microbiomes to land use at different phylogenetic scales. To test this, we compared patterns in temporal change for Shannon diversity for the different amplicons and found that a three-way interaction between amplicon, land use and season shapes temporal dynamics (three-way interaction Wald X^2 = 15.4, p = 0.02, Fig. 3G, Supp. Table R15). At the community level (i.e., *16S* and *ITS*), we saw few trends within land use types, except for consistent decreases in alpha diversity within forests in the spring. At the strain level, we found that *Pseudomonas* alpha diversity tended to decrease over sampling periods for all land use types. The pattern was less clear for *Sphingomonas*, in which alpha diversity increased in the Spring across all land use types in the first, but not second, year of our study. There were no effects of land use or season on alpha diversity of the fungal or bacterial microbiomes in the soil or companion plants (Supp. Fig. R13, Supp. Table R16); recall that we did not investigate *Sphingomonas* or *Pseudomonas* diversity in these sample types. Finally, we examined correlations between load and Shannon diversity to understand how land use affected these two aspects of microbial variation. Shannon diversity and load were weakly correlated for bacterial microbiomes, with the direction of the correlation differing between land use types (interaction Wald X^2 = 13.0, p = 0.001, Supp. Fig. R14, Supp. Table R17). For fungal microbiomes, a strong negative correlation was observed between

Shannon diversity and load, but without an effect of land use ($\beta = -1.04 \pm 0.06$ SE, $p < 0.0001$, Supp. Fig. R14, Supp. Table R17). Taken together, we conclude that season and land use structure the alpha-diversity of endophytic communities within *A. thaliana* endophytes, with differing impacts at microbial species versus strain levels, but no obvious effect for the soil and companion plant microbiomes.

The phyllosphere is assembled through microbial dispersal from the air, soil, and other co-occurring plants [36]. If land use is impacting the potential for microbial spillover from other sources, then we would expect to see associations between microbes in *A. thaliana* and microbes in companion plants or soil. We first examined this at the macro-community level to understand how the companion plant community affected *A. thaliana* microbial diversity. Indeed, companion plant community diversity, and thus the potential diversity of microbial sources, and *A. thaliana* endophyte bacterial and fungal diversity were positively correlated, but the correlation differed between land use types (bacterial interaction Wald $X^2 = 8.55$, $p = 0.01$; fungal interaction Wald $X^2 = 6.49$, $p = 0.04$; Supp. Table R18); there was no interaction with season. For bacteria, a positive correlation was observed for all land use types, but was steeper for anthropogenic sites (Fig. 4A). For fungi, the positive correlation was only observed in forest populations (Fig. 4B). Furthermore, *A. thaliana* microbial Shannon diversity was correlated with both microbial diversity from companion plants and soil, but the effects of land use and season differed between bacteria and fungi (Supp. Fig. R15, Supp. Table R19).

Next, we assessed microbial sharing between sample types using correlations for the dominant bacterial taxa in endophytes, Sphingomonadaceae, across land use types and seasons. We compared *A. thaliana* microbes with those in companion plants because of the detected effect of companion plant community diversity on microbial diversity (Fig. 4A), and also with soil microbes because of the strong effect of land use (Fig. 3D). We did not include fungi because the dominant taxa varied across sample types more than in bacterial microbiomes, resulting in insufficient sample sizes to make correlations. Each sample type displayed unique patterns of seasonal change across the land use types (Supp. Fig. R16) with seasonal fluctuations consistently observed only in endophytic Sphingomonadaceae. Sphingomonadaceae relative abundance in endophytes depended on its relative abundance in companion plants, but was shaped by a three-way interaction with season and land use (interaction Wald $X^2 = 15.0$, $p = 0.0006$, Fig. 4C, Supp. Table R20). A negative correlation was observed in the fall for sites with strong anthropogenic influence, which changed to a positive correlation in the spring; we observed the opposite pattern for forest and railroad populations. Endophyte-soil (Supp. Fig. R17) did not display the three-way interaction for Sphingomonadaceae, but two-way interactions between land use and season explained significant variance (Fig. 4D, Supp. Table R20); no significant association was observed for soil-companion plant correlations. Overall, we observe that the strength and direction of microbial sharing differed across seasons and land use types at different levels of organization, from the macro-plant community to microbial diversity to Sphingomonadaceae relative abundance.

Microbial abundance and diversity are associated with disease dynamics, but vary across land use types

353 In general, variance in disease PC1, which represents the number of symptoms, was better
354 explained by bacterial diversity and load, while disease PC2, which represents the symptom
355 types, was better explained by fungal load. Associations between bacterial load and disease
356 PC1, depended on land use type and season (Fig. 5A, Supp. Table R21). As mentioned
357 previously disease PC1 was higher in the spring ($\beta = 0.27 \pm 0.06$ SE, $p < 0.001$, Fig. 5A). Land
358 use type modified the relationship between disease PC1 and bacterial load (two-way interaction
359 Wald $X^2 = 6.7030$, $p = 0.03$, Fig. 5A). For example, forest populations tended to have consistent
360 bacterial loads across disease PC1, while anthropogenic and railroad populations were more
361 variable. Additionally, disease PC1 was negatively correlated with bacterial Shannon diversity,
362 with more symptoms observed in the plant associated with lower diversity (Fig. 5B). Companion
363 plant community diversity still explained significant variance when accounting for bacterial
364 effects on disease PC1 (Supp. Table R21). For disease PC2, fungal load-season interactions
365 explained significant variance for disease PC2 (interaction Wald $X^2 = 10.0$, $p = 0.002$, Fig. 5C,
366 Supp. Table R22), with a stronger and negative correlation in the fall.
367
368 These analyses show the importance of considering multiple facets of microbial diversity (e.g.,
369 load and diversity from bacteria and fungi) to explain patterns in disease dynamics. Importantly,
370 we find diversity at both the community and microbial level to be associated with reduced
371 disease, highlighting how processes across ecological scales potentially impact disease
372 dynamics.
373
374 ***DISCUSSION***
375 Here, we surveyed wild populations of *A. thaliana* across fall and spring seasons for disease
376 symptoms and microbiome variation. While other studies typically focus on microbiomes or
377 disease in the field, our study integrates both to show how land use impacts disease by
378 modulating different aspects of the microbiome. Disease was primarily shaped by interactions
379 between season and land use. In the spring, more individuals display multi-disease symptoms,
380 with higher microbial load and changes to microbial community composition (Figs. 2-3).
381 Increased companion plant community diversity was associated with reduced occurrence of
382 multiple disease symptoms, but this relationship differed between land use types (Fig. 4).
383 Intriguingly, plant community diversity was positively associated with increased *A. thaliana*
384 microbial diversity (Fig.4), and this higher microbial diversity was also associated with reduced
385 disease in *A. thaliana* (Fig. 5). Our results highlight how land use change can impact multiple
386 types of ecological interactions that in turn can change disease risk in wild populations.
387
388 We observed that higher biodiversity at two ecological scales–the plant community and within
389 the *A. thaliana* microbiome–resulted in less disease. This result is suggestive of the dilution
390 effect, where higher host diversity dilutes the disease risk in a multi-host pathogen system
391 [1,37,38]. Biodiversity loss associated with urban and agricultural environments often results in
392 communities enriched for species with life history traits associated with fast pace-of-life and
393 reduced investment in immune defenses, increasing the risk of disease spillover [3,38]. While
394 we did not measure these traits in the companion plant communities, land use types differed in
395 the correlation between disease symptoms and plant diversity (Fig. 2D) as well as plant
396 community composition (Supp. Fig. R3), suggesting that traits underlying the diversity-disease

397 relationship vary across land use types. The impact of this variation in disease-relevant plant
398 traits can also be further modulated by the abiotic factors, such as soil chemical properties [20].
399 Higher diversity microbiomes often provide greater protection against pathogens in plants
400 [7,9,39], as we observed here as well, but this protection also partially depends on microbial
401 load (Fig. 5). Protection by diverse microbiomes occurs when commensals saturate the host
402 niche space and consume resources that effectively outcompete invading pathogens [40,41].
403 Identifying potential synergies between the mechanisms underlying the dilution effect at the
404 plant community scale and within the microbiome is an important research priority.
405
406 Our results are consistent with several scenarios, but we believe that the following is particularly
407 attractive. First, plant community diversity protects against disease through plant traits that
408 dilute the community-level disease burden. In turn, increases in plant community diversity also
409 promote diversity within the *A. thaliana* microbiome, resulting in increased protection and
410 reduced disease. Additional support is required for this hypothetical scenario, preferably from
411 targeted manipulation of microbiomes, pathogens and companion plants. We note that the
412 dilution effect often depends on the spatial scale over which these interactions occur [42,43], but
413 it remains an open question how to apply the framework of the dilution effect to host-associated
414 microbiomes [1,42].
415
416 The concomitant increase in diversity between plant community and microbial diversity with
417 increased microbial diversity in *A. thaliana* exposes a tension in the diversity-disease
418 relationship. This diversity-begets-diversity relationship has been observed in a range of host
419 systems, including *A. thaliana* [15,38,44], but primarily for pathogens rather than commensal
420 microbes. The positive relationship between plant community and microbial diversity appeared
421 to be beneficial in our setting, but it also potentially amplifies disease risk by exposure to novel
422 microbes. Microbial sharing between host species is expected to accelerate microbial evolution
423 particularly under environmental change [5,45], but whether cross-species transmission
424 differentially impacts pathogens compared to commensal microbes is an open question.
425 Intriguingly, the correlation of Sphingomonadaceae between *A. thaliana* endophytes and the
426 other sample types suggests that land use alters microbial sharing (Fig. 4C-D).
427 Sphingomonadaceae abundance is often protective against bacterial pathogens [46,47], but as
428 we did not assess disease in companion plants, we do not know if this occurred in the surveyed
429 plants. A key research priority is to link how these different eco-evolutionary forces shape the
430 microbial evolution in wild host-microbe systems.
431
432 While it is tempting to attribute the negative relationship between microbial diversity and disease
433 to protection provided by the microbiome or the dilution effect operating at the microbial scale,
434 we do not know microbiome diversity prior to infection and thus cannot attribute causality.
435 Furthermore, we failed to detect strong effects of disease on structuring the beta-diversity of the
436 endophytic microbiome (Supp. Fig. D1), suggesting that microbial taxa did not consistently differ
437 between healthy and sick individuals. One issue is that pathogens often share the same 16S
438 rRNA sequence as non-pathogenic microbes in plant disease systems, such as in the *P.*
439 *syringae* complex [48], and so we have limited insight from our amplicon sequencing to identify
440 pathogens. We attempted to use the *HSD* amplicon for *Pseudomonas* genera, but we did not

find any associations in diseased plants (Supp. Fig. D2), suggesting this amplicon lacks sufficient resolution to identify pathogenic strains. While there may be technical limitations, Shannon diversity was the primary difference for the microbiome between healthy and diseased plants, leaving much of the variation in disease-microbiome interactions unexplained.

It is remarkable that so many *A. thaliana* individuals were observed to have multiple disease symptoms, and understanding this resilience of *A. thaliana* to disease pressure remains a key question. While multi-pathogen systems are common in the wild ecosystems, individuals seem to rarely experience strong negative effects of coinfection [12,13], which is aligned with our observations here. Additionally, infections did not appear to cost *A. thaliana* in growth or reproduction, as larger plants tended to have more disease symptoms and were just as likely to be bolting as healthy plants (Supp. Fig. D3). Note, however, that we did not measure phenotypes more directly associated with fitness. It is possible that disease symptoms may not necessarily be independent, as the same pathogen can cause multiple symptom types [49]. We cannot confirm the association between the number of symptoms, type of symptoms, and the number of pathogens due to the lack of resolution in amplicon sequencing. The disease symptoms observed here may not be due solely to disease, but may reflect exposure to environmental stress. Diagnosing the causative agents of symptoms combined with transcriptomic profiling would provide clarity into the relationship between land use and disease in *A. thaliana*.

Finally, it is important to consider the role of plant genetics and demography in shaping interactions between pathogens and the microbiome. Host genetics impacts microbiome composition in *A. thaliana* [18,32,35,50,51] as well disease resistance [51–54]. Land use in turn impacts host genetics, as different urban environments filter for different *A. thaliana* genotypes [55]. *Arabidopsis thaliana* has been shown to locally adapt to the companion plant community, particularly for alleles in immunity genes [19]. Railroads are implicated in increasing gene flow in a closely related species, *A. arenosa [56]*. Whether this applies to the *A. thaliana* populations here remains unknown, especially whether the introduced alleles by railroad-assisted gene flow would be associated with host control over the microbiome or disease resistance in the populations sampled. Both studies of urban adaptation [55] and introgression facilitated by railroads [56] identified selection on alleles associated with life-history traits that shorten the life cycle. Changes to the demography of *A. thaliana* across different land use types may lead to multiple cohorts of germination during each growing season. If these germination cohorts differ from the temporal dynamics of pathogen exposure, then this may explain seasonal differences in both the individual symptoms (Supp. Fig. R4) and composite disease scores (Fig. 2C) observed across land use types. Repeated sampling at smaller time intervals would help elucidate how temporal variation in pathogen exposure intersects with *A. thaliana* genetic variation and demography.

In conclusion, our results highlight the multitude of ways that land use change affects ecological interactions, from the macro-community level down to within-host microbial variation to plant disease dynamics. For the many ecological communities impacted by rapid anthropogenic change, our work here highlights the importance of understanding the interaction between

seasonality and ecological context that will shape disease dynamics in natural populations. Harnessing these interactions will be critical in developing the microbiome as a potential solution to provide protection against pathogens in wild and agricultural settings.

490 **Table 1: Top three most abundant microbes for each sample type**

	Bacteria
Endophyte	Sphingomonadaceae (33.7%), Oxalobacteraceae (15.9%), Comamonadaceae (8.5%)
Companions	Sphingomonadaceae (25.4%), Oxalobacteraceae (10.3%), Comamonadaceae (8.7%)
Soil	Sphingomonadaceae (13.4%), Actinobacteria (6.3%), Beijerinckiaceae (5.6%)
	Fungi
Endophyte	Mycosphaerellaceae (15.2%), Amphisphaeriaceae (13.5%), Helotiaceae (9.1%)
Companions	Didymellaceae (13.0%), Mycosphaerellaceae (10.5%), Cladosporiaceae (7.2%)
Soil	Nectriaceae (10.6%), Trichomeriaceae (5.3%), Helotiaceae

491
492

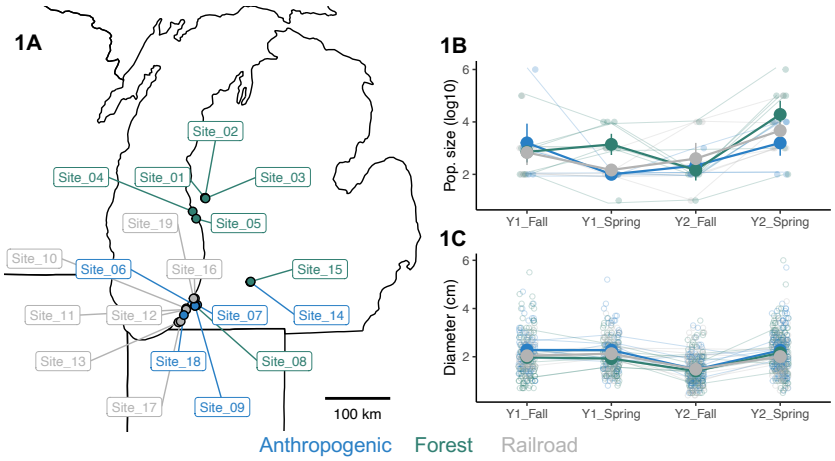

Fig. 1: Survey of *A. thaliana* populations. A) Map of populations near Lake Michigan, USA, color-coded by land use. B) Population size across seasons, colored by land use type. C) Size of individual plants across seasons. For B and C, smaller hollow circles and thin lines represent each population, while solid larger circles, thick lines represent the average from each land use category, with standard error.

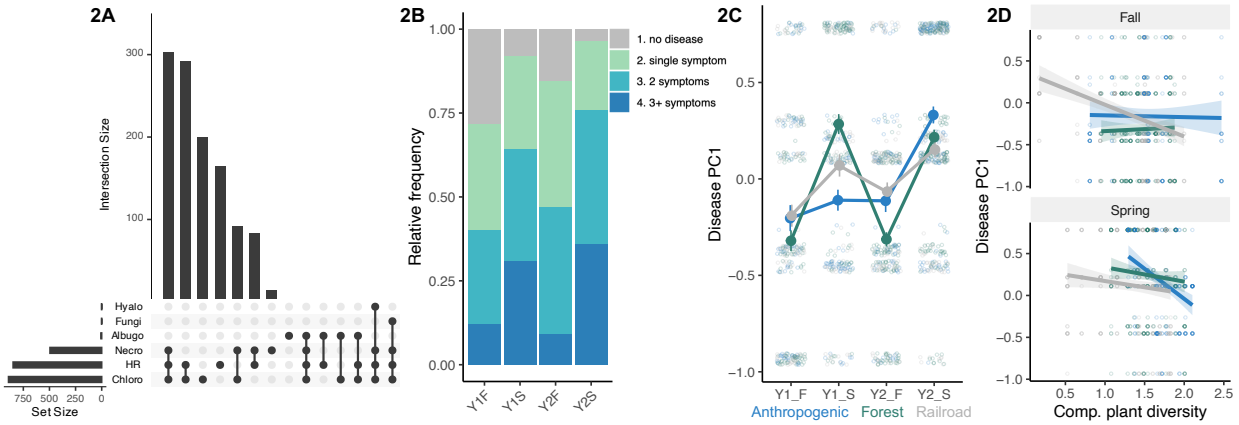

Fig. 2: Interactions between land use and season shape disease dynamics. A) Upset plot showing the overlap between different disease symptoms and counts across all plants sampled. B) Relative frequency of plants with the number of symptoms observed. C) Temporal dynamics in disease dynamics as indicated by the first principal component of the composite disease score. Smaller hollow circles represent individual plants, while the larger solid circles and thick lines represent the average from each land use category per season, with standard error. D) Companion plant community diversity is negatively correlated with disease PC1, but depends on land use and season. Small points represent individual plants, colored by land use.

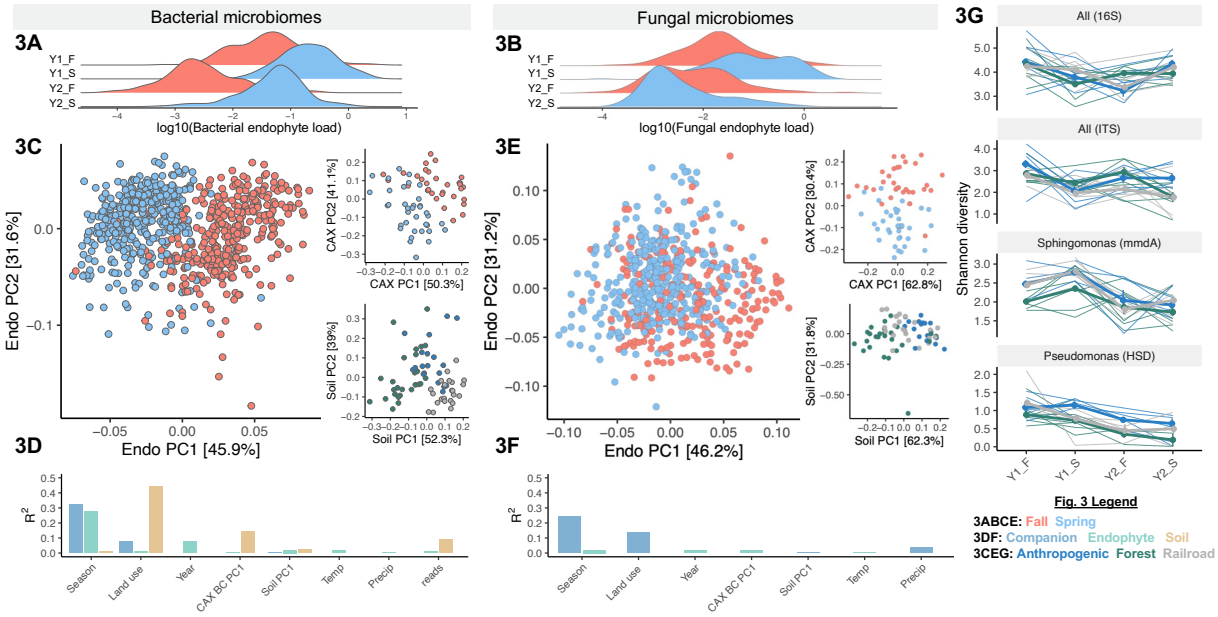

Fig. 3: Season and land use impact microbiomes across sample types. A) Bacterial load in spring (blue) and fall (red). B) Fungal load in spring and fall. C) Ordinations for bacterial microbiomes in *A. thaliana* endophytes, companion plants (abbreviated as "CAX"), and soil based on modified Aitchison distance matrix. Points are colored by the variable that explained the most variance. D) Bar plots of the R^2 value of each factor in PERMANOVA analysis for bacterial microbiomes, with color representing sample type (CAX BC PC1 = plant community beta-diversity using Bray-Curtis PCoA Axis 1). E) Ordinations for fungal microbiomes, colored by variables that explained the most variance. F) Bar plots of the R^2 value of each factor in PERMANOVA analysis for fungal microbiomes, with color representing sample type. No significant variance as explained by any factor for soil microbiomes. 3G) Shannon diversity of each amplicon across the four sampling seasons, colored by land use. Thin lines represent each population, while thick lines and solid circles show mean, with standard error.

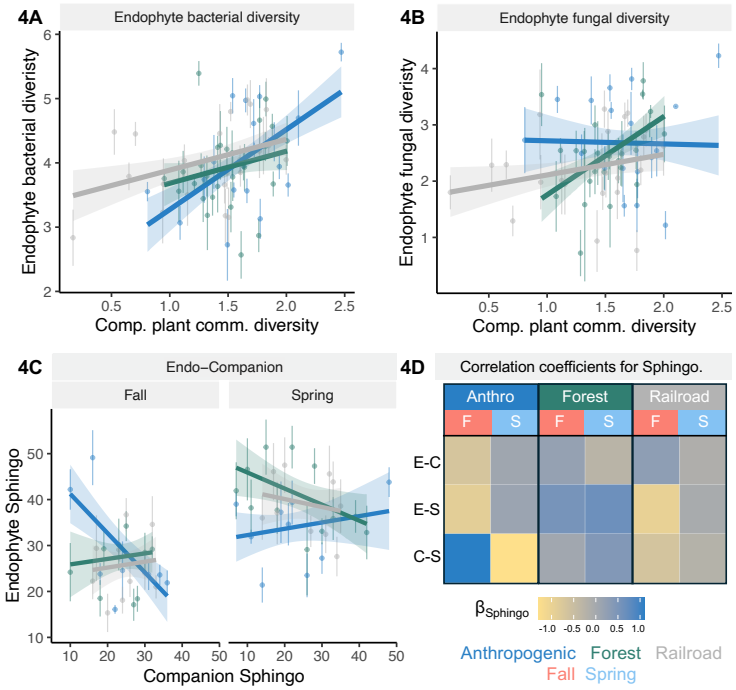

Fig. 4: Land use impacts microbial diversity and sharing between sample types. For A-C, points represent the correlation between companion plant and mean (+/- standard error) for relative abundance in the endophytes for each population, colored by land use. A) *Arabidopsis thaliana* endophyte microbial diversity is positively correlated with the companion plant community diversity, but the slope differs between land use types. B) *Arabidopsis thaliana* fungal diversity is also positively correlated with companion plant community diversity, but not for anthropogenic sites. C) Correlations for the relative abundance of the dominant bacterial family, Sphingomonadaceae, between companion plant and *A. thaliana* endophyte microbiomes. Other sample types are in Supp. Fig. R17. D) Boxes represent the Sphingomonadaceae correlation coefficients (β) for a given sample type pair. Y-axis titles are abbreviated comparisons for E-C: endophyte-companion, E-S: endophyte-soil, and C-S: companion-soil.

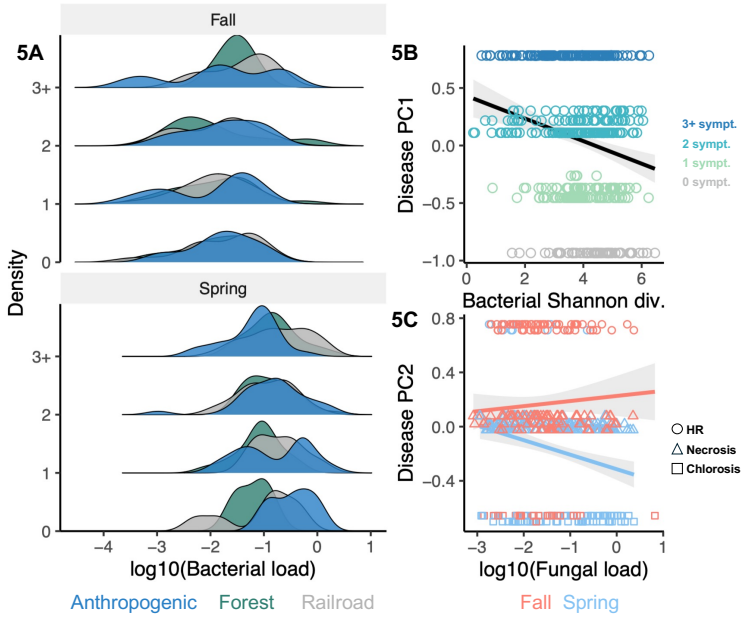

Fig. 5: Associations between microbiome variation and disease symptoms are shaped by season and land use. A) Associations between bacterial load and disease PC1 as a function of land use type and season. Density plots reflect the number of individuals for a given disease PC1 (i.e., multiple-symptom class), colored by land use type. B) Association of Shannon diversity bacterial microbiomes with disease PC1 scores, with points colored by the number of symptoms observed. C) Association of fungal load with disease PC2, with points colored by season and shape reflecting symptom type associated with PC2 score.

552 ***REFERENCES***

553 1. Keesing F *et al.* 2010 Impacts of biodiversity on the emergence and transmission of
554 infectious diseases. *Nature* **468**, 647–652.

555 2. Baker RE *et al.* 2022 Infectious disease in an era of global change. *Nat. Rev. Microbiol.* **20**,
556 193–205.

557 3. Laine A-L. 2023 Plant disease risk is modified by multiple global change drivers. *Curr. Biol.*
558 **33**, R574–R583.

559 4. Jones KE, Patel NG, Levy MA, Storeygard A, Balk D, Gittleman JL, Daszak P. 2008 Global
560 trends in emerging infectious diseases. *Nature* **451**, 990–993.

561 5. McDonald BA, Stukenbrock EH. 2016 Rapid emergence of pathogens in agro-ecosystems:
562 global threats to agricultural sustainability and food security. *Philos. Trans. R. Soc. Lond. B*
563 *Biol. Sci.* **371**. (doi:10.1098/rstb.2016.0026)

564 6. Parker IM, Saunders M, Bontrager M, Weitz AP, Hendricks R, Magarey R, Suiter K, Gilbert
565 GS. 2015 Phylogenetic structure and host abundance drive disease pressure in
566 communities. *Nature* **520**, 542–544.

567 7. Berg M, Koskella B. 2018 Nutrient- and Dose-Dependent Microbiome-Mediated Protection
568 against a Plant Pathogen. *Curr. Biol.* **28**, 2487–2492.e3.

569 8. Fitzpatrick CR, Salas-González I, Conway JM, Finkel OM, Gilbert S, Russ D, Teixeira
570 PJPL, Dangl JL. 2020 The plant microbiome: From ecology to reductionism and beyond.
571 *Annu. Rev. Microbiol.* **74**, 81–100.

572 9. Wang NR, Wiesmann CL, Melnyk RA, Hossain SS, Chi M-H, Martens K, Craven K, Haney
573 CH. 2021 Commensal Pseudomonas fluorescens Strains Protect Arabidopsis from Closely
574 Related Pseudomonas Pathogens in a Colonization-Dependent Manner. *MBio* **13**,
575 e0289221.

576 10. Henry LP, Bruijning M, Forsberg SKG, Ayroles JF. 2021 The microbiome extends host
577 evolutionary potential. *Nat. Commun.* **12**, 5141.

578 11. Henry LP, Bergelson J. 2023 Evolutionary implications of host genetic control for
579 engineering beneficial microbiomes. *Curr Opin Syst Biol* **34**, None.

580 12. Stukenbrock EH, McDonald BA. 2008 The origins of plant pathogens in agro-ecosystems.
581 *Annu. Rev. Phytopathol.* **46**, 75–100.

582 13. Alexander HM. 2010 Disease in natural plant populations, communities, and ecosystems:
583 Insights into ecological and evolutionary processes. *Plant Dis.* **94**, 492–503.

584 14. Tollenaere C, Susi H, Laine A-L. 2016 Evolutionary and epidemiological implications of
585 multiple infection in plants. *Trends Plant Sci.* **21**, 80–90.

586 15. Bartoli C *et al.* 2018 In situ relationships between microbiota and potential pathobiota in
587 Arabidopsis thaliana. *ISME J.* **12**, 2024–2038.

588 16. Emmenegger B, Massoni J, Pestalozzi CM, Bortfeld-Miller M, Maier BA, Vorholt JA. 2023

589 Identifying microbiota community patterns important for plant protection using synthetic
590 communities and machine learning. *Nat. Commun.* **14**, 7983.

591 17. In press. National Land Cover Database Class Legend and Description. See
592 https://www.mrlc.gov/data/legends/national-land-cover-database-class-legend-and-
593 description (accessed on 10 June 2025).

594 18. Roux F, Frachon L, Bartoli C. 2023 The genetic architecture of adaptation to leaf and root
595 bacterial Microbiota in Arabidopsis thaliana. *Mol. Biol. Evol.* **40**.
596 (doi:10.1093/molbev/msad093)

597 19. Frachon L, Mayjonade B, Bartoli C, Hautekèete N-C, Roux F. 2019 Adaptation to Plant
598 Communities across the Genome of Arabidopsis thaliana. *Mol. Biol. Evol.* **36**, 1442–1456.

599 20. Roux F, Frachon L. 2022 A Genome-Wide Association study in Arabidopsis thaliana to
600 decipher the adaptive genetics of quantitative disease resistance in a native heterogeneous
601 environment. *PLoS One* **17**, e0274561.

602 21. Lundberg DS, Pramoj Na Ayutthaya P, Strauß A, Shirsekar G, Lo W-S, Lahaye T, Weigel
603 D. 2021 Host-associated microbe PCR (hamPCR) enables convenient measurement of
604 both microbial load and community composition. *Elife* **10**. (doi:10.7554/eLife.66186)

605 22. Bolyen E *et al.* 2019 Reproducible, interactive, scalable and extensible microbiome data
606 science using QIIME 2. *Nat. Biotechnol.* **37**, 852–857.

607 23. McMurdie PJ, Holmes S. 2013 phyloseq: an R package for reproducible interactive analysis
608 and graphics of microbiome census data. *PLoS One* **8**, e61217.

609 24. Callahan BJ, McMurdie PJ, Rosen MJ, Han AW, Johnson AJA, Holmes SP. 2016 DADA2:
610 High-resolution sample inference from Illumina amplicon data. *Nat. Methods* **13**, 581–583.

611 25. Bokulich NA, Kaehler BD, Rideout JR, Dillon M, Bolyen E, Knight R, Huttley GA, Gregory
612 Caporaso J. 2018 Optimizing taxonomic classification of marker-gene amplicon sequences
613 with QIIME 2's q2-feature-classifier plugin. *Microbiome* **6**. (doi:10.1186/s40168-018-0470-z)

614 26. McDonald D, Price MN, Goodrich J, Nawrocki EP, DeSantis TZ, Probst A, Andersen GL,
615 Knight R, Hugenholtz P. 2012 An improved Greengenes taxonomy with explicit ranks for
616 ecological and evolutionary analyses of bacteria and archaea. *ISME J.* **6**, 610–618.

617 27. Abarenkov K *et al.* 2024 The UNITE database for molecular identification and taxonomic
618 communication of fungi and other eukaryotes: sequences, taxa and classifications
619 reconsidered. *Nucleic Acids Res.* **52**, D791–D797.

620 28. Martino C, Morton JT, Marotz CA, Thompson LR, Tripathi A, Knight R, Zengler K. 2019 A
621 novel sparse compositional technique reveals microbial perturbations. *mSystems* **4**.
622 (doi:10.1128/mSystems.00016-19)

623 29. Bates D, Sarkar D, Bates MD, Matrix L. 2007 The lme4 package. *R package version* **2**, 74.

624 30. Hartig. 2024 DHARMa: Residual Diagnostics for Hierarchical (Multi-Level / Mixed)
625 Regression Models.

626 31. Oksanen J *et al.* 2015 Vegan community ecology package: ordination methods, diversity

627 analysis and other functions for community and vegetation ecologists. *R package ver* , 2–3.

628 32. Horton MW *et al.* 2014 Genome-wide association study of Arabidopsis thaliana leaf
629 microbial community. *Nat. Commun.* **5**, 5320.

630 33. Almario J, Mahmoudi M, Kroll S, Agler M, Placzek A, Mari A, Kemen E. 2022 The leaf
631 microbiome of Arabidopsis displays reproducible dynamics and patterns throughout the
632 growing season. *MBio* **13**, e0282521.

633 34. Lundberg DS *et al.* 2022 Contrasting patterns of microbial dominance in the Arabidopsis
634 thaliana phyllosphere. *Proc. Natl. Acad. Sci. U. S. A.* **119**, e2211881119.

635 35. Karasov TL *et al.* 2024 Continental-scale associations of Arabidopsis thaliana phyllosphere
636 members with host genotype and drought. *Nat. Microbiol.* **9**, 2748–2758.

637 36. Vorholt JA. 2012 Microbial life in the phyllosphere. *Nat. Rev. Microbiol.* **10**, 828–840.

638 37. Keesing F, Holt RD, Ostfeld RS. 2006 Effects of species diversity on disease risk: Effects of
639 species diversity on disease risk. *Ecol. Lett.* **9**, 485–498.

640 38. Halliday FW, Rohr JR, Laine A-L. 2020 Biodiversity loss underlies the dilution effect of
641 biodiversity. *Ecol. Lett.* **23**, 1611–1622.

642 39. Hu J, Wei Z, Kowalchuk GA, Xu Y, Shen Q, Jousset A. 2020 Rhizosphere microbiome
643 functional diversity and pathogen invasion resistance build up during plant development.
644 *Environ. Microbiol.* **22**, 5005–5018.

645 40. Spragge F, Bakkeren E, Jahn MT, B N Araujo E, Pearson CF, Wang X, Pankhurst L,
646 Cunrath O, Foster KR. 2023 Microbiome diversity protects against pathogens by nutrient
647 blocking. *Science* **382**, eadj3502.

648 41. Schäfer M, Pacheco AR, Künzler R, Bortfeld-Miller M, Field CM, Vayena E, Hatzimanikatis
649 V, Vorholt JA. 2023 Metabolic interaction models recapitulate leaf microbiota ecology.
650 *Science* **381**, eadf5121.

651 42. Rohr JR, Civitello DJ, Halliday FW, Hudson PJ, Lafferty KD, Wood CL, Mordecai EA. 2020
652 Towards common ground in the biodiversity-disease debate. *Nat. Ecol. Evol.* **4**, 24–33.

653 43. Keesing F, Ostfeld RS. 2021 Dilution effects in disease ecology. *Ecol. Lett.* **24**, 2490–2505.

654 44. Johnson PTJ, Wood CL, Joseph MB, Preston DL, Haas SE, Springer YP. 2016 Habitat
655 heterogeneity drives the host-diversity-begets-parasite-diversity relationship: evidence from
656 experimental and field studies. *Ecol. Lett.* **19**, 752–761.

657 45. Thines M. 2019 An evolutionary framework for host shifts - jumping ships for survival. *New*
658 *Phytol.* **224**, 605–617.

659 46. Vogel C, Bodenhausen N, Gruissem W, Vorholt JA. 2016 The Arabidopsis leaf
660 transcriptome reveals distinct but also overlapping responses to colonization by
661 phyllosphere commensals and pathogen infection with impact on plant health. *New Phytol.*
662 **212**, 192–207.

663 47. Vogel CM, Potthoff DB, Schäfer M, Barandun N, Vorholt JA. 2021 Protective role of the

664 Arabidopsis leaf microbiota against a bacterial pathogen. *Nat. Microbiol.* **6**, 1537–1548.

665 48. Karasov TL *et al.* 2018 Arabidopsis thaliana and Pseudomonas Pathogens Exhibit Stable
666 Associations over Evolutionary Timescales. *Cell Host Microbe* **24**, 168–179.e4.

667 49. Katagiri F, Thilmony R, He SY. 2002 The Arabidopsis thaliana-pseudomonas syringae
668 interaction. *Arabidopsis Book* **1**, e0039.

669 50. Bergelson J, Brachi B, Roux F, Vailleau F. 2021 Assessing the potential to harness the
670 microbiome through plant genetics. *Curr. Opin. Biotechnol.* **70**, 167–173.

671 51. Brachi B *et al.* 2022 Plant genetic effects on microbial hubs impact host fitness in repeated
672 field trials. *Proc. Natl. Acad. Sci. U. S. A.* **119**, e2201285119.

673 52. Barrett LG, Kniskern JM, Bodenhausen N, Zhang W, Bergelson J. 2009 Continua of
674 specificity and virulence in plant host-pathogen interactions: causes and consequences.
675 *New Phytol.* **183**, 513–529.

676 53. Todesco M *et al.* 2010 Natural allelic variation underlying a major fitness trade-off in
677 Arabidopsis thaliana. *Nature* **465**, 632–636.

678 54. Karasov TL *et al.* 2014 The long-term maintenance of a resistance polymorphism through
679 diffuse interactions. *Nature* **512**, 436–440.

680 55. Schmitz G *et al.* 2024 Environmental filtering of life-history trait diversity in urban
681 populations of *Arabidopsis thaliana*. *J. Ecol.* **112**, 14–27.

682 56. Baduel P, Hunter B, Yeola S, Bomblies K. 2018 Genetic basis and evolution of rapid cycling
683 in railway populations of tetraploid Arabidopsis arenosa. *PLoS Genet.* **14**, e1007510.

684